frontiers in Energy Research

ORIGINAL RESEARCH
published: 17 February 2022
doi: 10.3389/fenrg.2022.847947

Experimental and Numerical Study on the Combustion Characteristics of a Laminar Non-Premixed Methane Jet Flame in Oxygen/Carbon Dioxide Coflow

Fan Zhang[1], *Xing Li*[2,3,4]*, *Shengrong Xie*[2,5], *Junxiong Wang*[2] and *Xiaohan Wang*[2]

[1]*School of Mechanical and Electric Engineering, Guangzhou University, Guangzhou, China,* [2]*Guangzhou Institute of Energy Conversion, Chinese Academy of Sciences, Guangzhou, China,* [3]*Dalian National Laboratory for Clean Energy, Dalian, China,* [4]*Department of Energy and Mechanical Engineering, Hunan Institute of Humanities, Science and Technology, Loudi, China,* [5]*University of Chinese Academy of Sciences, Beijing, China*

OPEN ACCESS

Edited by:
Zhihua Wang, Zhejiang University, China

Reviewed by:
Yu Wang, Wuhan University of Technology, China
Lei Zhou, Harbin Institute of Technology, Shenzhen, China
Jinhua Wang, Xi'an Jiaotong University, China

***Correspondence:**
Xing Li
lixing@ms.giec.ac.cn
inspirationlee@hotmail.com

Specialty section:
This article was submitted to Advanced Clean Fuel Technologies, a section of the journal Frontiers in Energy Research

Received: *03 January 2022*
Accepted: *24 January 2022*
Published: *17 February 2022*

Citation:
Zhang F, Li X, Xie S, Wang J and Wang X (2022) Experimental and Numerical Study on the Combustion Characteristics of a Laminar Non-Premixed Methane Jet Flame in Oxygen/Carbon Dioxide Coflow. Front. Energy Res. 10:847947. doi: 10.3389/fenrg.2022.847947

The combustion characteristics of laminar non-premixed CH_4 jet flame in an O_2/CO_2 coflows with different oxygen mole fractions were studied experimentally. The flame heights at different oxygen concentrations and fuel jet velocity were obtained. The experimental observation shows that the luminosity of the CH_4 jet flame in O_2/CO_2 coflow is different from that of the flame in air stream. A two-dimensional numerical study of a laminar non-premixed CH_4 jet flame in the O_2/CO_2 coflow with the O_2 mole fraction of 0.35 was conducted to analyze the effects of CO_2 dilution on the flame. The distribution of OH radicals in the flame was measured experimentally using planar laser-induced fluorescence (PLIF) to validate the computational method adopted in this work, and the computational and experimental results of the OH distributions showed good consistency at various fuel flow velocities. Three artificial species were created in the numerical experiment to analyze the effects of the chemical reactions, third-body collisions, and transport properties of CO_2 on the height, width, and temperature distribution of the flame. The results showed that CO_2 participation in chemical reactions exerts significant effects on the flame. However, the influences of the third-body effects and transport properties of CO_2 on the jet flame are unremarkable. The global reaction pathways and distributions of important species in the laminar non-premixed CH_4 jet flame were analyzed in detail to investigate the influence mechanisms of CO_2 on the flame height and temperature. The entire flame can be divided into two oxidation parts, which separated by the boundary of the HCCO. The H, O, and OH concentrations and distributions in different parts of the flame were influenced by CO_2 dilution, resulting in different flame heights and temperature distributions.

Keywords: non-premixed laminar jet flame, O_2/CO_2 coflow, chemical effect, third-body effect, transport property

INTRODUCTION

The reduction of CO_2 emissions during fossil fuel utilization is an important task for human society. The injection of purified CO_2 from flue gas into underground reservoirs is believed to help achieve this goal (Buhre et al., 2005; Wall, 2007). However, CO_2-rich flue gas is required to increase the efficiency and economy during carbon capture and storage. Several new advanced combustion technologies that use O_2/CO_2 as an oxidizer, such as oxy-fuel combustion technology (Buhre et al., 2005; Wall, 2007; Hjärtstam et al., 2009; Rathnam et al., 2009; Scheffknecht et al., 2011; Taniguchi et al., 2011; Chen et al., 2012; Dhaneswar and Pisupati, 2012; Luo et al., 2015; Moroń and Rybak, 2015; Liu et al., 2016; Ge et al., 2017; Seddighi, 2017; Menage et al., 2018; Zhang et al., 2018), moderate or intense low-oxygen dilution (MILD) oxy-combustion (Li et al., 2013; Tu et al., 2015; Mardani and FazlollahiGhomshi, 2016; Mao et al., 2017; Gładysz et al., 2018), gaseous fuel-fired oxy-fuel combustion technology (Yin et al., 2011; Seepana and Jayanti, 2012a; Seepana and Jayanti, 2012b; Oh et al., 2013a; Oh et al., 2013b; Oh and Noh, 2013; Oh and Noh, 2014; Giménez-López et al., 2015; Oh and Noh, 2015; Oh and Hong, 2016; Bürkle et al., 2018), and high-temperature oxygen combustion technology (Li et al., 2014; Li et al., 2015; Li et al., 2016), have been developed to meet this requirement. However, many other challenges must be solved before these combustion technologies can be widely adopted in the industry, since the differences in the physical properties and chemical characteristics of CO_2 and N_2 can lead to important distinctions in flame structure. More information on the combustion characteristics of different fuels in various O_2/CO_2 environments must be obtained for the development of new combustion approaches.

Experimental and numerical studies on the fundamental combustion characteristics of O_2/CO_2-fired flames have been conducted previously. The effect of CO_2 on the free-propagation speed of laminar premixed $CH_4/O_2/CO_2$ flames was investigated numerically (Liu et al., 2003). The speeds of laminar $CH_4/O_2/CO_2$ flames at different equivalence ratios and pressures were measured and computed (Xie et al., 2013). The CH_4 oxidation under CO_2-rich conditions has also been investigated using an atmospheric pressure flow reactor (Glarborg and Bentzen, 2008). The effects of environmental pressure (Maruta et al., 2007) and oxidizer temperature (Li et al., 2014) on the stretch extinction characteristics of CH_4/CO_2 versus O_2/CO_2 counterflow non-premixed flames have been studied through experiments and numerical computations. The ignition temperature of a stoichiometric $CH_4/O_2/CO_2$ mixture was examined by using a micro flow reactor with a controlled temperature profile (Li et al., 2015). The fundamental studies (Liu et al., 2003; Maruta et al., 2007; Glarborg and Bentzen, 2008; Xie et al., 2013; Li et al., 2014; Li et al., 2015; Li et al., 2016) show that CO_2 exerts an inhibitory effect on flames. Consequently, a higher oxygen concentration is recommended for the O_2/CO_2-fired flames to achieve a comparable combustion characteristics as the air flames.

The previous fundamental studies have provided an essential understanding of flames in O_2/CO_2 environments (Liu et al., 2003; Maruta et al., 2007; Glarborg and Bentzen, 2008; Xie et al., 2013; Li et al., 2014; Li et al., 2015; Li et al., 2016). However, the three-dimensional structures of flames in O_2/CO_2, which are important for the development of industrial burner, deserves more attention. The combustion characteristics of turbulent premixed CH_4/air/CO_2 and $CO/H_2/CO_2/O_2$ flames was investigated experimentally (Kobayashi et al., 2007; Kobayashi et al., 2009; Wang et al., 2013). And it was observed that local wrinkled structures become sharp and propagate deeply into the burned mixture with addition of CO_2. It was also proposed that CO_2 addition is effective for restraining combustion oscillation (Kobayashi et al., 2007). Experimental studies of the swirl-stabilized turbulent CH_4/air and $CH_4/O_2/CO_2$ flames show that the average length of air flames is longer than that of oxy-flames. Moreover, it was found that one-dimensional laminar flame properties could not be used to explain the intense burning of turbulent oxy-flames (Watanabe et al., 2016).

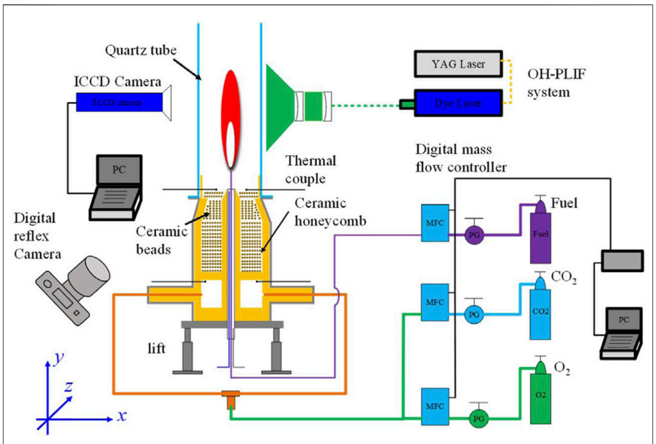

FIGURE 1 | Schematic of the experimental system.

Recently, the influences of CO_2 on the combustion characteristics of multidimensional flames has been studied in detail. The physical and chemical effects of CO_2 dilution on a CH_4/H_2 jet flame in the MILD oxy-combustion regime have been investigated using two-dimensional numerical computations with a detailed kinetic mechanism (Tu et al., 2016; Tu et al., 2017). It was found that the chemical effects of CO_2 play a comparable role in the suppression of temperature rise to the physical effects (Tu et al., 2016). The influences of CO_2 dilution on the shape and structure of laminar CO/H_2 diffusion flames in an $O_2/N_2/CO_2$ coflow was examined (Xu et al., 2017), and the chemical effects of the thermal and transport properties of CO_2 on the flames were discussed in detail. The previous numerical studies provide important information on the effects of CO_2 under MILD (Tu et al., 2016; Tu et al., 2017) and syngas (Xu et al., 2017) combustion regimes. However, the effects of CO_2 on the flame shape and temperature distribution of gaseous-fuel-fired flames in an O_2/CO_2 environment with a high O_2 concentration needs special attention and was not clarified.

The target of the present work is to study on the combustion characteristics of laminar non-premixed methane jet flames in oxygen/carbon dioxide coflows. The laminar flame heights at different oxygen concentrations were measured by experiments. The OH distributions of typical laminar methane jet flames in a O_2/CO_2 coflow were measured by OH-PLIF technique. Two-dimensional numerical computations with a detailed kinetic mechanism were conducted, and three artificial species modified from CO_2 were employed in the numerical experiment to clarify the effects of CO_2. The influences through the chemical reactions, third-body collisions, and transport properties of CO_2 on the combustion characteristics of a laminar non-premixed CH_4 jet flame in an O_2/CO_2 environment with a high O_2 concentration was distinguished in detail.

EXPERIMENT

Experimental Setup and Method

Figure 1 shows a schematic diagram of the experimental system. The jet-flame experimental apparatus includes three parts, namely, a quartz tube, a fuel tube, and a stainless-steel chamber. The length and height of the rectangular quartz tube are 10 and 60 cm, respectively, and the wall thickness is 4 mm. The fuel stream was supplied through a stainless-steel tube with an inner diameter (d) of 1 mm and a length of 15 cm. The fuel tube was installed at the center of a rectangular quartz tube. The rectangular quartz tube and the stainless-steel chamber were connected together, and a ceramic honeycomb (diameter, 12 cm; height, 10 cm) and ceramic beads (diameter, 2 mm) were arranged in the stainless-steel chamber to achieve a uniform coflow velocity. A well-mixed O_2/CO_2 stream was fed into the rectangular quartz tube from the bottom of the chamber. Three MKS digital mass flow controllers were employed to control the volumetric flow rates of gases, and a wet gas meter (Shinagawa, W-NK-2) was used to calibrate the digital mass flow controllers. The rectangular quartz tube was adopted in the experiment because it is convenient for optical measurements. In addition, the similarity of non-premixed laminar CH_4 jet flames in a circular tube with an inner diameter of 9.2 cm to those in a rectangular quartz tube has been confirmed by preliminary experiment. The laminar CH_4 jet flames in O_2/CO_2 colfows with different oxygen mole fractions (X_{O2} = 0.30, 0.35 and 0.40) were tested by the present experimental system.

A single-lens reflex digital camera (Nikon D-610, f/4) was fixed in front of the flame to record the flame images. The ISO and exposure time were set as 1,250 and 1/40 s, respectively. The qualitative distribution of OH radicals in laminar non-premixed CH_4 jet flames in an O_2/CO_2 coflow was measured using the OH-PLIF technique. The experimental apparatus was fixed on a lifter with a scale which can adjust the position of the flame. Consequently, the OH distribution of the different parts of the flame can be measured. The distribution of OH radicals at the center plane of the flame was measured by the OH-PLIF system. A beam with a wavelength of 355 nm was provided by a Nd:YAG laser (Quanta-Ray Pro-230). This beam was then transformed into a new laser beam by a dye laser (Sirah PSCAN-G-30) to excite the OH radicals in the flame. The wavelength of the dye laser beam was around 283.565 nm for the present OH-PLIF system. And the height of the laser sheet was about 40 mm and the thickness was less than 100 μm at the location of the flame. An ICCD camera (LAVISION VC-IRO and VC-Imager Pro X 4M) with an OH filter was used to obtain the OH image of the flame. The finest pixel resolution of the ICCD camera at the flame position was approximately 50 μm. A detailed description of the OH-PLIF system and the selected wavelength is provided elsewhere (Li et al., 2017). Raw OH-PLIF images were directly used for qualitative comparison with the numerical results because the measured OH intensity is proportional to the computational OH molar concentration within a 10% error (Yamamoto et al., 2009). The OH-PLIF results at each fuel flow velocity were averaged from every 100 OH-PLIF images. As the length of the laser sheet at the location of the flame was approximately 40 mm, which cannot cover the overall scope of the flame, the OH distributions in different parts of the flame were measured by adjusting the height of the experimental apparatus. The overall OH distribution of a jet flame was assembled from the OH distributions at different parts of the flame.

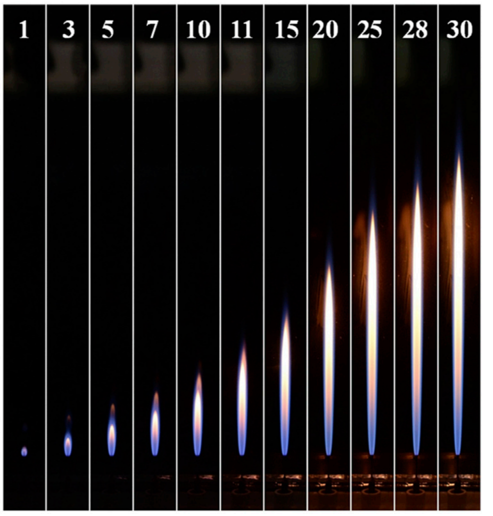

FIGURE 2 | The images of CH_4-jet-flames in O_2/CO_2 coflows with an oxygen mole fraction of 0.35. (The number on the top denotes the corresponding fuel flow velocity in the unit of m/s).

Experimental Results

The flame height and width which are determined by oxygen concentration and fuel flow rate are important parameter for the design of the industrial burner. Consequently, the laminar CH_4 jet flames in O_2/CO_2 coflows with oxygen mole fractions (X_{O2}) of 0.30, 0.35 and 0.40 were studied experimentally. The coflow velocity was kept at 0.1 m/s for different cases. The laminar CH_4 jet flames in the air coflow were also tested for the comparison. The images of CH_4 laminar jet flames in the O_2/CO_2 coflow (X_{O2} = 0.35) with different fuel jet velocities are shown in **Figure 2**. It can be seen that the flame height of the laminar CH_4 jet flame increase linearly with the fuel velocity when the O_2/CO_2 is used as the oxidizer.

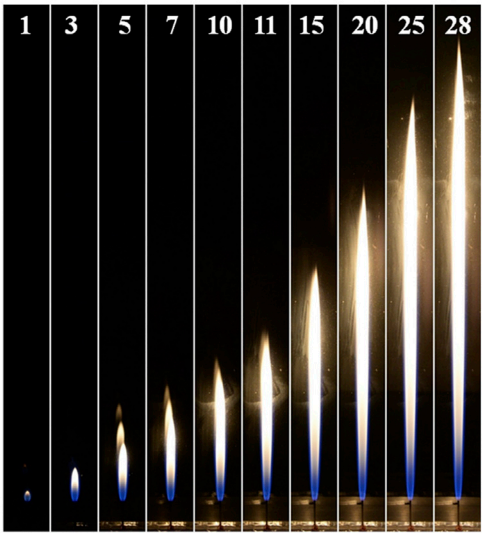

FIGURE 3 | The images of CH_4-jet-flames in air coflow. (The number on the top denotes the corresponding fuel flow velocity in the unit of m/s).

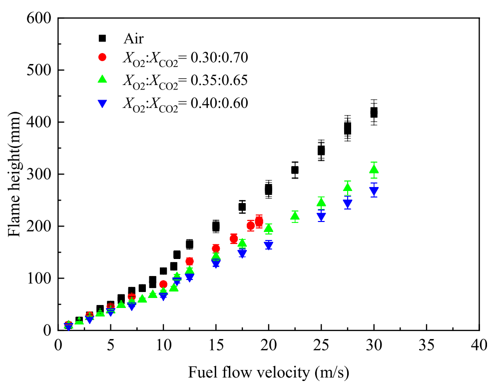

FIGURE 4 | Measured flame heights of CH_4-jet-flames in O_2/CO_2 and air coflows with 5% error bars.

The experimental results in **Figures 2, 3** show that the luminosity of the flame in the O_2/CO_2 coflow is different from that of the laminar CH_4 jet flame in air. Both the laminar CH_4 jet flames in the air and O_2/CO_2 coflows can be divided into two sections, bottom and top partitions, based on the flame luminosity. The bottom section of the flame is dominated by the blue color luminosity, while the top partition of flame shows orange and yellow colors for the flame in O_2/CO_2 and air respectively. It can be seen that the bottom section of the flame with O_2/CO_2 coflow show dark blue color, however, the flame in air is more bright. The luminosities of the laminar CH_4 jet flames in O_2/CO_2 and air coflows suggests that the effect of CO_2 on the flame structure is remarkable, which needs further investigation.

The flame height of laminar CH_4 jet flames in O_2/CO_2 (X_{O2} = 0.30, 0.35 and 0.40) and air coflows were measured, as shown in

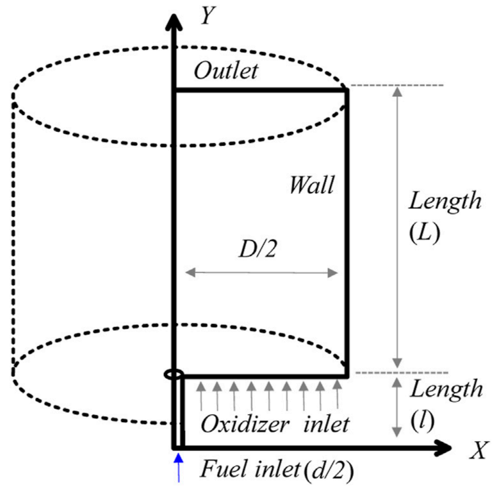

FIGURE 5 | Physical model and boundary conditions.

Figure 4. It can be seen that the flame height is smoothly decreased as the increase of oxygen mole fraction. The flame in air is taller than those of the flames in O_2/CO_2 coflows. The theoretical study on the flame length of non-premixed laminar jet flame was conducted in the early studies (Roper, 1977; Roper et al., 1977), and the formula of the flame length for circular port burner was obtained and shown as follows,

$$L_f = \frac{Q\left(T_0/T_F\right)}{4\pi D_0 \ln\left(1+\frac{1}{S}\right)}\left(T_0/T_f\right)^{0.67} \quad (1)$$

Where T_0, T_F and T_f are the ambient temperature, the fuel flow temperature and the average temperature of the flame respectively. Q is the volumetric flow rate of fuel stream, S is the stoichiometric molar ratio of oxidizer to fuel. D_0 is the diffusion coefficient at T_0. The increase of oxygen concertation leads a decrease of the stoichiometric molar ratio of oxidizer to fuel and an increase of the flame temperature. Consequently the laminar flame height in the O_2/CO_2 coflow with a higher oxygen concentration is lower.

NUMERICAL COMPUTATION AND ANALYSIS

Physical Model and Computation Method

Numerical computation with a detailed reaction mechanism was conducted to clarify the effects of CO_2 on the combustion characteristics of the laminar CH_4 jet flame in O_2/CO_2 colfow. **Figure 5** illustrates the physical model and boundary conditions. A CH_4 stream was injected into the O_2/CO_2 coflow through a tube with an inner diameter (d) of 1 mm and a length (L) of 15 cm. The length (L) and width (D/2) of the computation domain are 50 and 4.6 cm, respectively. An O_2/CO_2 mixture with an O_2 mole fraction (X_O) of 0.35 was used in the study, since the previous work has shown that the counterflow non-premixed CH_4 flame in an O_2/CO_2 coflow with X_O = 0.35 has a combustion

TABLE 1 | Properties of artificial species.

	KCO_2	XCO_2	DCO_2
Chemical effect as CO_2	×	×	√
Third-body effects as CO_2	√	×	√
Thermal properties as CO_2	√	√	√
Transport properties as CO_2	√	√	×

intensity comparable with that of an air flame (Maruta et al., 2007; Li et al., 2014). The pressure in the system was 1 atm, and the inlet temperature of the oxidizer and fuel streams was 300 K. Laminar non-premixed CH_4 jet flames with two different fuel jet velocities (V_F = 5 and 10 m/s, Re = 293 and 586) were investigated. The inlet flow velocity of the oxidizer stream was fixed at 0.1 m/s. The laminar non-premixed jet flame was simplified to a two-dimensional axisymmetric swirl model. All walls were considered to be in a no-slip state. A convective heat transfer boundary (ambient temperature, 300 K; convective heat transfer coefficient, 6 W/m^2·K) based on the experimental conditions was used for the wall of the computational domain, and an adiabatic wall condition was applied to the fuel tube wall. While the velocity inlet boundary was used at the fuel and oxidizer inlets, the pressure outlet boundary was applied at the outlet.

The governing equations included the mass, momentum, energy, and species-conservation equations, as well as the ideal gas equation of state. A detailed description of the governing equations can be found elsewhere (Li et al., 2017). The governing equations were discretized based on the finite-volume method, and the open-source framework, OpenFOAM (OpenFOAM, 2016) was employed to conduct the numerical study. The SIMPLE algorithm was used. The finite rate chemistry model and the GRI-Mech 3.0 mechanism (Smith et al., 2020) were also used to compute the chemical reactions. Previous studies on CO_2-diluted flames (Liu et al., 2003; Maruta et al., 2007; Xie et al., 2013; Li et al., 2014; Li et al., 2015) have shown satisfactory performance of the mechanism. The diffusion coefficient was calculated using the Maxwell–Stefan equations. The thermal diffusion effect was also included in the calculations. Mesh independence was confirmed by preliminary numerical computations. Grids with 136320 cells were used, and the finest grid size was 45 μm. The values of 1.0×10^{-6} and 1.0×10^{-8} were used as convergence criteria for the mass and energy conservation equations and chemical reactions, respectively. Radiation heat transfer from the gases was not included in the computation, since the present work primarily focuses on comparisons of the effects of the chemical reactions, third-body collisions, and transport properties of CO_2. A discussion on the radiation of CO_2 on non-premixed flames can be found elsewhere (Maruta et al., 2007).

Additional computations using three artificial species modified from CO_2 were conducted to analyze the effects of the chemical reactions, third-body reactions, and transport properties of CO_2 on the combustion characteristics of the laminar non-premixed jet flame. The properties of the artificial species are listed in **Table 1**. The first artificial species is KCO_2, which does not participate in chemical reactions but participates in third-body collisions and has thermal and transport properties identical to those of CO_2. The second artificial species is XCO_2, which has the same thermal and transport properties as CO_2 but does not participate in chemical reactions and third-body collisions. The third artificial species is DCO_2, which has the same chemical reactions, third-body effects, and thermal properties as CO_2 but transport properties (i.e., thermal conductivities, viscosities, diffusion coefficients,

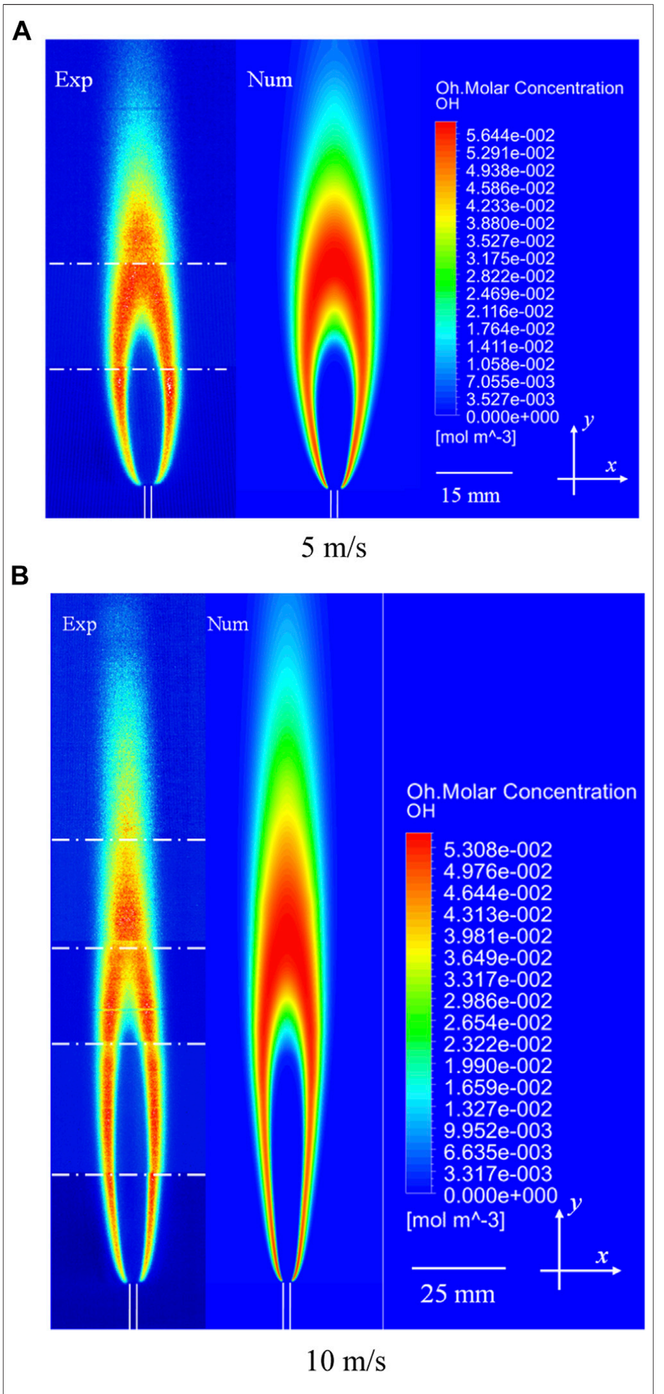

FIGURE 6 | Measured and computated OH distributions of laminar non-premixed CH_4 jet flames in an O_2/CO_2 coflow at fuel jet velocities of 5 and 10 m/s. **(A)** 5 m/s. **(B)** 10 m/s.

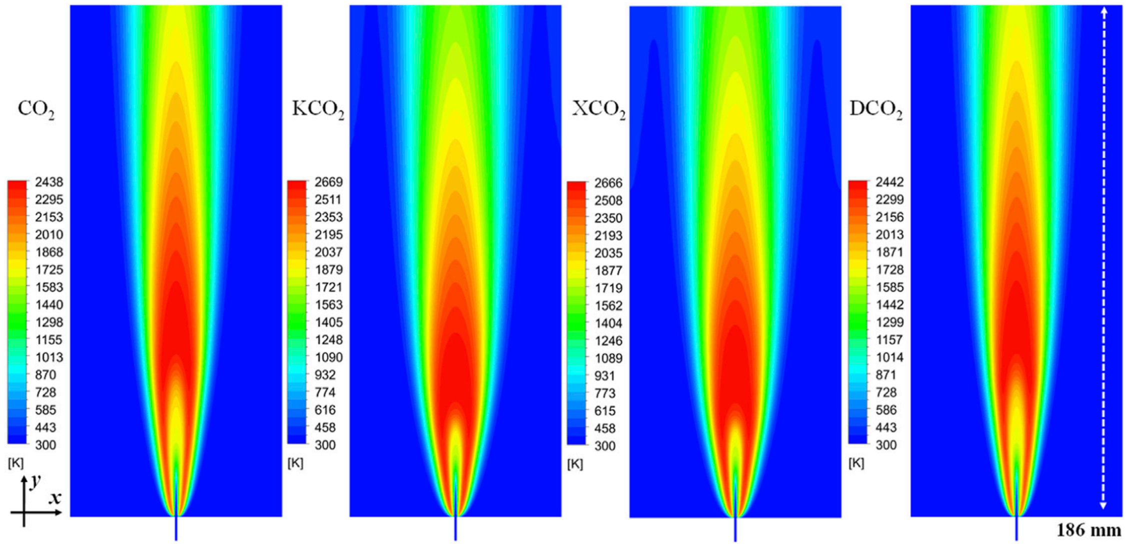

FIGURE 7 | Computational temperature distributions in flames in different oxidizers (V_F = 10 m/s).

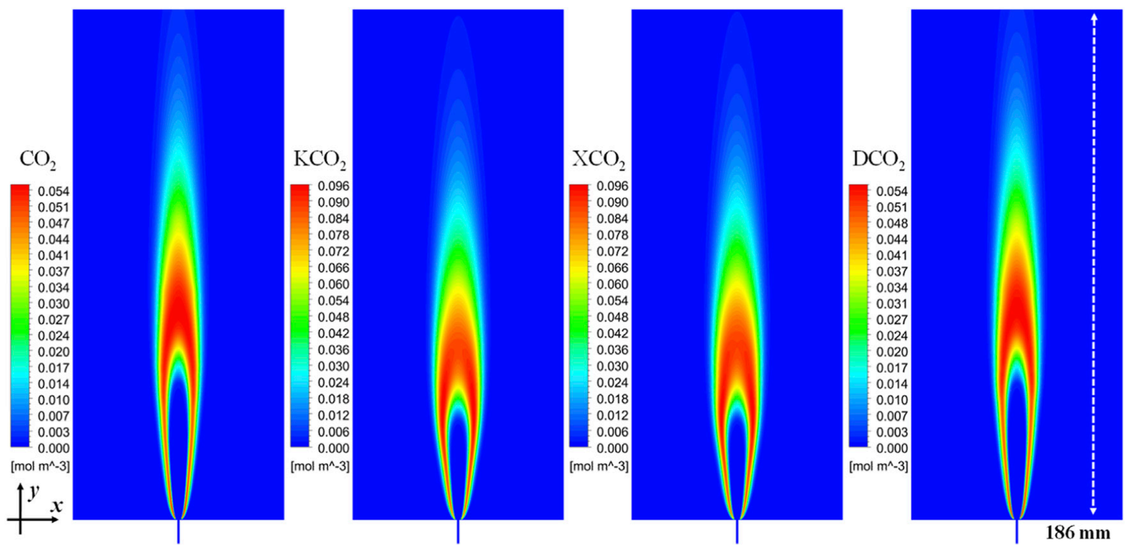

FIGURE 8 | Computational OH radical distributions in flames in different oxidizers (V_F = 10 m/s).

and thermal diffusion coefficients) identical to those of N_2. The participation or not of CO_2 in the chemical reactions can lead to differences in the computational results between the CO_2 and KCO_2 conditions. Differences in the combustion characteristics between KCO_2 and XCO_2 can be attributed to the third-body effects of CO_2. The effects of the transport properties of CO_2 on the jet flame can be attributed to differences in the computational results between the DCO_2 and CO_2 cases.

Validation of the Computational Method

The computational OH distributions of laminar non-premixed CH_4 jet flames at V_F = 5 and 10 m/s were compared with the experimental results, as shown in **Figure 6**. The total OH distributions in the flames at fuel jet velocities of 5 and 10 m/s consist of three and five parts, respectively. It can be seen that the shape and height determined from the computational OH distributions are consistent with the results obtained from the experiment. The small difference between the computational and experimental OH distributions may be attributed to two reasons: the laser sheet is not perfectly set at the center of the flame and is slightly inclined and the computational method assumes a two-dimensional physical model and neglects radiation heat loss. Despite minor differences can be observed between the measured and computational OH distributions, the

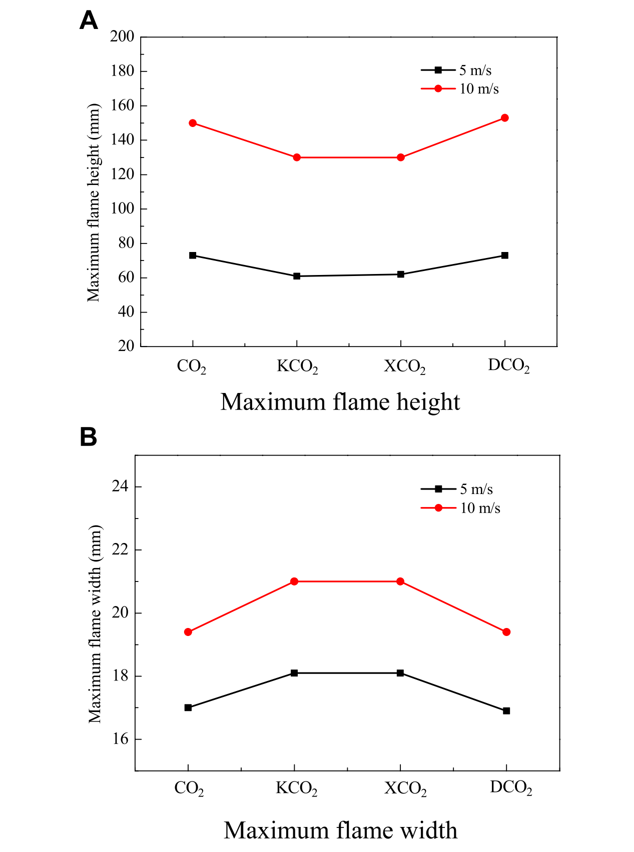

FIGURE 9 | Computational flame height and width based on OH distributions in laminar non-premixed CH_4 jet flames in different oxidizers. **(A)** Maximum flame height. **(B)** Maximum flame width.

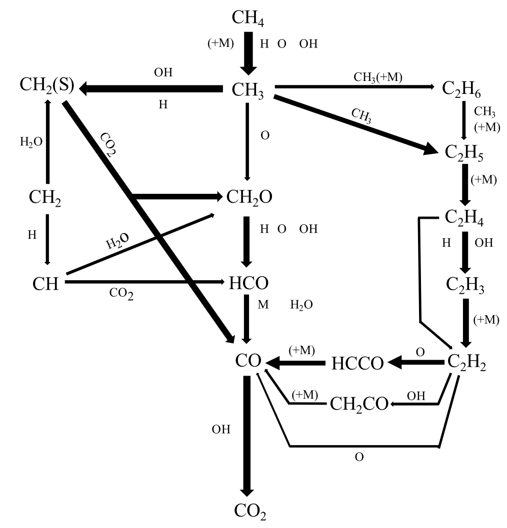

FIGURE 10 | Integral reaction flow in a laminar non-premixed CH_4 jet flame in an O_2/CO_2 coflow at V_F = 10 m/s (thick lines show the major reactions).

comparison of the overall results indicates that the present computational method and kinetic mechanism are reasonable for the study of the effects of CO_2 on the combustion characteristics of laminar non-premixed CH_4 jet flames in an O_2/CO_2 coflow with a high O_2 concentration.

Effects of CO_2 on Flame Temperature and Shape

The computational results of jet flames in O_2/CO_2, O_2/KCO_2, O_2/XCO_2, and O_2/DCO_2 coflows were obtained and compared. **Figures 7**, **8** respectively show the temperature and OH distributions in laminar non-premixed jet flames at V_F = 10 m/s. The flames in the O_2/CO_2 and O_2/DCO_2 coflows are nearly identical, and the flames in O_2/KCO_2 and O_2/XCO_2 coflows are almost the same. Comparison of flames in the O_2/KCO_2 and O_2/XCO_2 coflows indicates that the contribution of the third-body effects of CO_2 on the shape and temperature distribution of the laminar jet flame is insignificant. The results of flames in the O_2/CO_2 and O_2/DCO_2 coflows reveal that the difference in transport properties between CO_2 and N_2 also does not lead to a significant change in the flames. However, the difference between the flames in the O_2/CO_2 and O_2/KCO_2 coflows suggests that the flame shape and temperature distribution of laminar non-premixed jet flames are significantly changed by the chemical effects of CO_2. Specifically, the flame height is decreased, whereas the maximum flame width is increased, when the chemical effects of CO_2 are excluded from consideration. The decrease in the maximum flame temperature by the chemical effect of CO_2 is approximately 230 K.

The detailed computational results of laminar non-premixed CH_4 jet flames in O_2/CO_2, O_2/KCO_2, O_2/XCO_2, and O_2/DCO_2 coflows at a fuel flow velocities of 5 and 10 m/s were analyzed. The flame heights and widths based on the OH distribution in flames in different oxidizers at V_F = 5 and 10 m/s are illustrated in **Figures 9A,B**, respectively. The flame boundaries are judged by 99% decrease of the maximum OH molar concentration. The variations in the flame height and width of laminar non-premixed CH_4 jet flames at V_F = 5 m/s in different oxidizer coflows are similar to those of flames at V_F = 10 m/s. Although not shown here, the numerical results indicate that the maximum flame temperatures at V_F = 5 m/s in O_2/CO_2 and O_2/DCO_2 are nearly identical, i.e., 2470 K, and the maximum flame temperatures in O_2/KCO_2 and O_2/XCO_2 are similar, i.e., approximately 2670 K. The computational OH distributions show that flame height decreases, whereas flame width increases, when the chemical effect of CO_2 is suspended.

Mechanism of CO_2 on the Laminar Non-Premixed CH_4 Jet Flames

The reaction pathways and flame structures in O_2/CO_2, O_2/KCO_2, O_2/XCO_2 and O_2/DCO_2 were analyzed to interpret the mechanism of the chemical effect of CO_2 on laminar non-premixed CH_4 jet flames. The primary reaction pathways of flames in the O_2/KCO_2, O_2/XCO_2, and O_2/DCO_2 coflows are nearly identical to those of flames in the O_2/CO_2 coflow.

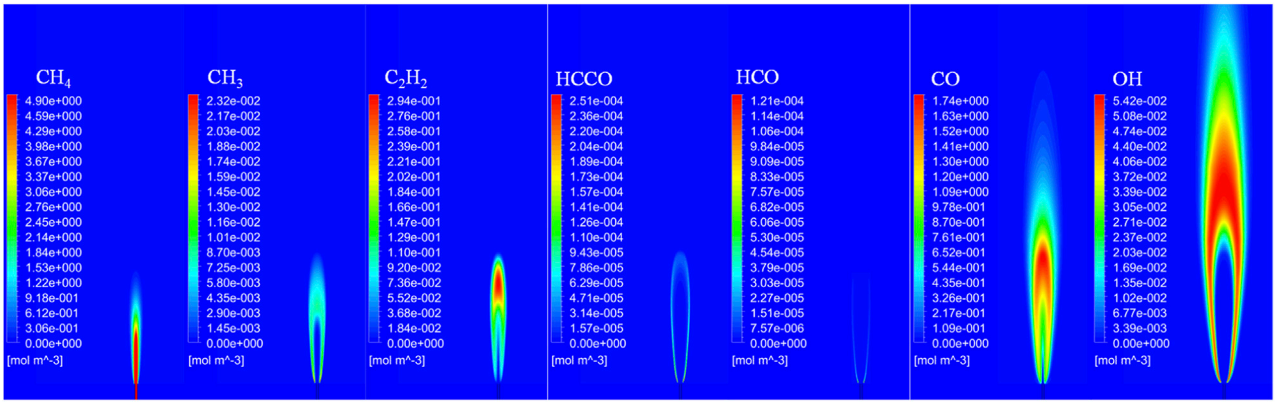

FIGURE 11 | Molar concentrations of important species in a laminar non-premixed CH_4 jet flame in an O_2/CO_2 coflow (V_F = 10 m/s).

Figure 10 shows the global reaction pathways of laminar non-premixed flames in the O_2/CO_2 coflow at V_F = 10 m/s. CH_4 is transformed into CH_3 through H abstraction by H, O, and OH. Most of the CH_3 radicals are transformed into C_2H_5, $CH_2(S)$, and C_2H_6, and only a small amount of the CH_3 radicals react with O atoms to produce CH_2O. Most of the C_2H_6 generated is transformed into C_2H_5 through third-body reactions. C_2H_5 radicals decompose rapidly into C_2H_4, and H abstraction by H and OH, which are important sources of C_2H_4 consumption, produces C_2H_3 radicals. The reaction $C_2H_3(+M) = C_2H_2 + H (+M)$ consumes C_2H_3 radicals to produce C_2H_2. Most of the C_2H_2 is consumed by reaction with O to produce HCCO. The HCCO radicals generate CH and CO via the third-body reaction $HCCO(+M) = CH + CO(+M)$. Finally, CO is oxidized to CO_2 by the reaction $OH + CO = H + CO_2$.

Figure 11 shows the distribution of important species in a laminar non-premixed jet flame in an O_2/CO_2 environment at V_F = 10 m/s. The CH_4-rich region can be observed near the exit of the tube, and the CH_3-rich region can be observed around the region with a high CH_4 concentration. The C_2H_2-rich concentration region is located at nearly the same area as the CH_3-rich region. The HCCO is found on the margins of the C_2H_2-rich region, and theHCO only exists at the two sides of the CH_3-rich region. The molar concentration of the HCCO is higher than that of the HCO. The CO-rich region is located downstream of the HCCO-rich region.

The analysis of the computational results of flames in the O_2/KCO_2, O_2/XCO_2, and O_2/DCO_2 coflows shows that the distributions of important species are similar to those of flames in O_2/CO_2. Moreover, laminar non-premixed CH_4 jet flames in different oxidizers can be divided into two parts based on the global oxidation process. The results of flames in the O_2/CO_2 coflow at V_F = 10 m/s are illustrated in **Figure 12**; here, the white dotted line indicates the boundary between the first and second parts of the flame. The first part of the flame includes the oxidation process from CH_4 to CO through the reaction pathway $CH_4 \rightarrow CH_3 \rightarrow C_2H_6 \rightarrow C_2H_5 \rightarrow C_2H_4 \rightarrow C_2H_3 \rightarrow C_2H_2 \rightarrow HCCO \rightarrow CO$, while the primary reaction in the second part is the oxidation of CO to CO_2. Consequently, the top of the HCCO region is used as the boundary separating the first and second parts of the flame. Generation of H_2 and H_2O is mainly completed in the first part of the flame. The distribution of the heats of reaction indicates that the first and second parts of the flame make remarkable contributions to heat generation. A distinct endothermic region is located in the first part of the flame. The effects of CO_2 on the first and second typical parts of non-premixed laminar jet flames result in different combustion characteristics.

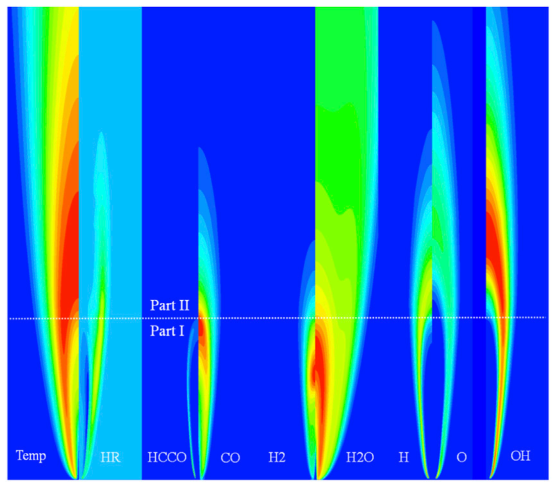

FIGURE 12 | The structure of the laminar non-premixed CH_4 jet flame (V_F = 10 m/s) in an O_2/CO_2 coflow. (Temp: temperature; HR: heat of reaction).

The distributions of important species of flames in the O_2/CO_2 and O_2/KCO_2 coflows were compared to enable interpretation of the chemical effect of CO_2 on the laminar non-premixed CH_4 jet flame, since the effect of third-body collisions with CO_2 on the laminar non-premixed jet flame has been confirmed to be negligible. The distributions of the molar concentrations of HCCO, CO, O, and H in the flames in O_2/CO_2 and O_2/KCO_2 coflows are shown in **Figures 13A–D**. The heights of the HCCO-, CO-, O-, and H-rich regions in the flame in the O_2/KCO_2 coflow

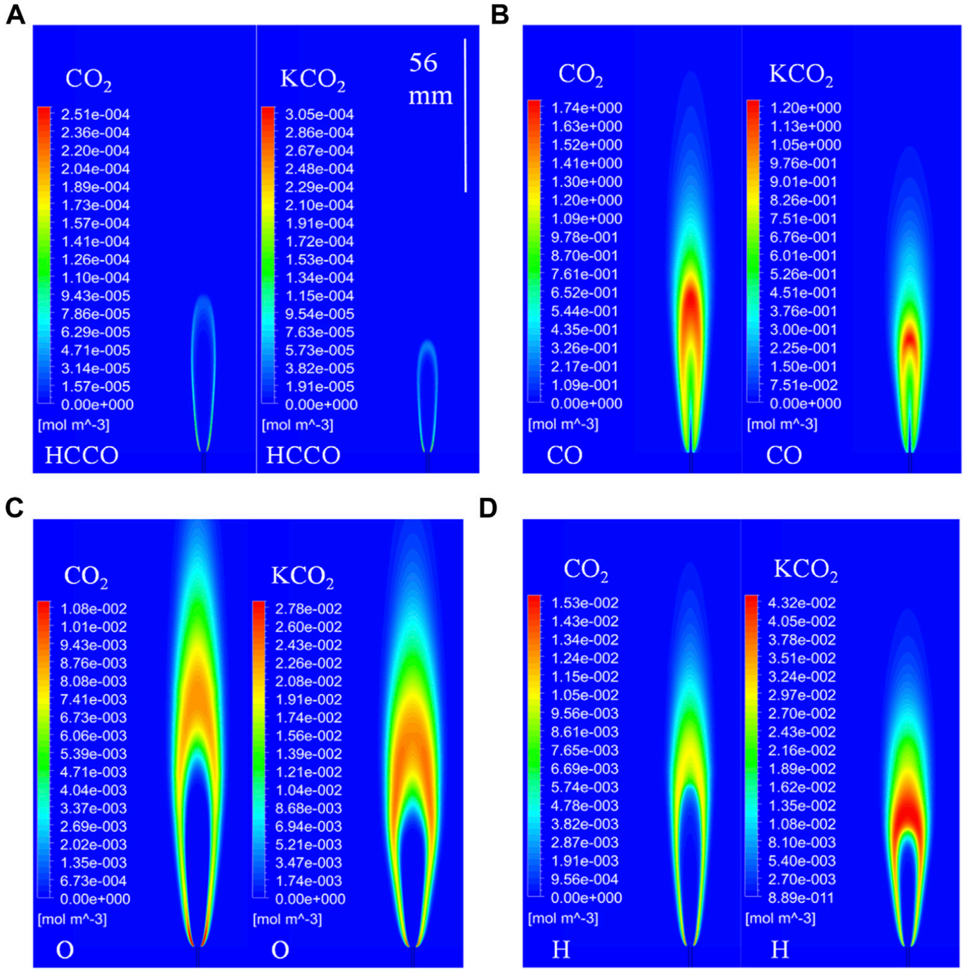

FIGURE 13 | Distributions of the molar concentration of important species in flames in O_2/CO_2 and O_2/KCO_2: **(A)** HCCO, **(B)** CO, **(C)** O, and **(D)** H.

are shorter than those in the flame in the O_2/CO_2 coflow. Interestingly, the difference between the heights of the HCCO-rich region in the flames in the O_2/CO_2 and O_2/KCO_2 coflows is nearly identical to that between the heights of the OH-rich regions (as shown in **Figure 8**). The difference between the flame heights based on the OH distribution is related to differences in HCCO distribution in the first part of the flame. The analysis of the reaction pathways shows that HCCO is primarily produced by the reaction O+ C_2H_2 = H + HCCO. As O atoms are mainly generated by the reaction H + O_2 = O+ OH, the flame height essentially depends on the H distribution. The contours of the H molar concentration shown in **Figure 13D** indicate that the concentration of H atoms of the flame in O_2/KCO_2 is significantly higher than that of the flame in O_2/CO_2. Pathway analysis of the entire flame region shows that the reaction OH + CO = H + CO_2 is an important source of H atoms. This finding suggests that the chemical effect of CO_2 on H formation and distribution ultimately leads to a difference in flame heights.

The results shown in **Figure 12** indicate that the high-temperature region and the OH-rich region are coincident, this finding can also be observed from the results shown in **Figures 7**, **8**. This phenomena is attributed to the fact that the high-temperature region is located in the second part of the laminar non-premixed flame, where the reaction OH + CO = H + CO_2 is the primary exothermic reaction. The results shown in **Figure 7** indicate that the maximum temperature of the laminar non-premixed flame in the O_2/CO_2 coflow is approximately 230 K lower than that of the flame in the O_2/KCO_2 coflow. Although not shown here, analysis of the computational results shows that the net reaction rates of OH + CO = H + CO_2 and H + O_2 = O + OH of the flame in the O_2/CO_2 coflow are lower than those of the flame in the O_2/KCO_2 coflow. The net reaction rate of OH + CO = H + CO_2 in the second part of the flame is significantly reduced by the chemical effect of CO_2, which results in a low flame temperature.

CONCLUSION

The heights of the laminar CH_4 jet flames in O_2/CO_2 coflows with different oxygen mole fractions of 0.30, 0.35 and 0.40 were obtained by experimental study. The height of the flame in

O_2/CO_2 coflow decreases as the increase of oxygen mole fraction. And the height of the laminar CH_4 jet flame in O_2/CO_2 coflow with oxygen mole fraction of 0.30 is shorter than that of the laminar CH_4 jet flame in air. Moreover, the luminosity of the CH_4 jet flame in O_2/CO_2 coflow is totally different from that of the flame in air stream.

The chemical reactions, third-body effects, and transport properties of CO_2 on the combustion characteristics of a laminar non-premixed CH_4 jet flame in an O_2/CO_2 coflow with a high O_2 concentration (X_O = 0.35) were investigated using a two-dimensional numerical computational method with a detailed kinetic mechanism. The computational OH distributions showed good consistency with the results obtained from the experiments. Whereas the third-body effect and transport properties of CO_2 do not exert remarkable effects on the laminar non-premixed flame, the chemical effect of CO_2 on the laminar non-premixed jet flame is significant. The chemical effect of CO_2 increases the flame height but decreases the maximum flame temperature. The primary oxidation pathway in the jet flame is $CH_4 \rightarrow CH_3 \rightarrow C_2H_6 \rightarrow C_2H_5 \rightarrow C_2H_4 \rightarrow C_2H_3 \rightarrow C_2H_2 \rightarrow HCCO \rightarrow CO \rightarrow CO_2$. The CH_4 non-premixed laminar jet flame can be divided into two parts based on the global oxidization process; here, the top of the HCCO-rich region is the boundary between these parts. The decrease in the concentration of O atoms by the chemical effect of CO_2 in the first part of the flame can explain the observed decrease in flame height, and the inhibitory effect of CO_2 on the reaction rate of OH + CO = H + CO_2 in the second part of the flame induces a decrease in maximum flame temperature.

DATA AVAILABILITY STATEMENT

The original contributions presented in the study are included in the article/supplementary material, further inquiries can be directed to the corresponding author.

AUTHOR CONTRIBUTIONS

FZ: Laser diagnostic, Data analysis, Reviewing and editing. XL: Conceptualization, Supervision, Methodology, Investigation, Reviewing and editing, Funding acquisition. SX: Data Curation, Reviewing and editing. JW: Data Curation, Reviewing and editing. XW: Reviewing and editing.

FUNDING

The supports of National Natural Science Foundation of China (No. 52176139) and the DNL Cooperation Fund, CAS (DNL202006) are gratefully acknowledged.

REFERENCES

Buhre, B. J. P., Elliott, L. K., Sheng, C. D., Gupta, R. P., and Wall, T. F. (2005). Oxy-fuel Combustion Technology for Coal-Fired Power Generation. *Prog. Energ. Combustion Sci.* 31, 283–307. doi:10.1016/j.pecs.2005.07.001

Bürkle, S., Dreizler, A., Ebert, V., and Wagner, S. (2018). Experimental Comparison of a 2D Laminar Diffusion Flame under Oxy-Fuel and Air Atmosphere. *Fuel* 212, 302–308. doi:10.1016/j.fuel.2017.10.067

Chen, L., Yong, S. Z., and Ghoniem, A. F. (2012). Oxy-fuel Combustion of Pulverized Coal: Characterization, Fundamentals, Stabilization and CFD Modeling. *Prog. Energ. Combustion Sci.* 38, 156–214. doi:10.1016/j.pecs.2011.09.003

Dhaneswar, S. R., and Pisupati, S. V. (2012). Oxy-fuel Combustion: The Effect of Coal Rank and the Role of char-CO2 Reaction. *Fuel Process. Technol.* 102, 156–165. doi:10.1016/j.fuproc.2012.04.029

Ge, X., Dong, J., Fan, H., Zhang, Z., Shang, X., Hu, X., et al. (2017). Numerical Investigation of Oxy-Fuel Combustion in 700°C-Ultra-Supercritical Boiler. *Fuel* 207, 602–614. doi:10.1016/j.fuel.2017.06.119

Giménez-López, J., Millera, A., Bilbao, R., and Alzueta, M. U. (2015). Experimental and Kinetic Modeling Study of the Oxy-Fuel Oxidation of Natural Gas, CH_4 and C_2H_6. *Fuel* 160, 404–412. doi:10.1016/j.fuel.2015.07.087

Gładysz, P., Stanek, W., Czarnowska, L., Sładek, S., and Szlęk, A. (2018). Thermo-ecological Evaluation of an Integrated MILD Oxy-Fuel Combustion Power Plant with CO_2 Capture, Utilisation, and Storage – A Case Study in Poland. *Energy* 144, 379–392. doi:10.1016/j.energy.2017.11.133

Glarborg, P., and Bentzen, L. L. B. (2008). Chemical Effects of a High CO_2 Concentration in Oxy-Fuel Combustion of Methane. *Energy Fuels* 22, 291–296. doi:10.1021/ef7005854

Hjärtstam, S., Andersson, K., Johnsson, F., and Leckner, B. (2009). Combustion Characteristics of lignite-fired Oxy-Fuel Flames. *Fuel* 88, 2216–2224. doi:10.1016/j.fuel.2009.05.011

Kobayashi, H., Hagiwara, H., Kaneko, H., and Ogami, Y. (2007). Effects of CO_2 Dilution on Turbulent Premixed Flames at High Pressure and High Temperature. *Proc. Combust. Inst.* 31, 1451–1458. doi:10.1016/j.proci.2006.07.159

Kobayashi, H., Yata, S., Ichikawa, Y., and Ogami, Y. (2009). Dilution Effects of Superheated Water Vapor on Turbulent Premixed Flames at High Pressure and High Temperature. *Proc. Combust. Inst.* 32, 2607–2614. doi:10.1016/j.proci.2008.05.078

Li, P., Dally, B. B., Mi, J., and Wang, F. (2013). MILD Oxy-Combustion of Gaseous Fuels in a Laboratory-Scale Furnace. *Combust. Flame* 160, 933–946. doi:10.1016/j.combustflame.2013.01.024

Li, X., Jia, L., Nakamura, H., Tezuka, T., Hasegawa, S., and Maruta, K. (2015). Study on Flame Responses and Ignition Characteristics of $CH_4/O_2/CO_2$ Mixture in a Micro Flow Reactor with a Controlled Temperature Profile. *Appl. Therm. Eng.* 84, 360–367. doi:10.1016/j.applthermaleng.2015.03.022

Li, X., Jia, L., Onishi, T., Grajetzki, P., Nakamura, H., Tezuka, T., et al. (2014). Study on Stretch Extinction Limits of CH_4/CO_2 versus High Temperature O_2/CO_2 Counterflow Non-premixed Flames. *Combust. Flame* 161, 1526–1536. doi:10.1016/j.combustflame.2013.12.004

Li, X., Yang, H., Jiang, L., Wang, X., and Zhao, D. (2016). Stretch Extinction Characteristics of CH_4/CO_2 versus $O_2/H_2O/CO_2$ and O_2/H_2O Counterflow Non-premixed Flames at Different Oxidizer Temperatures. *Fuel* 186, 648–655. doi:10.1016/j.fuel.2016.09.017

Li, X., Zhang, J., Yang, H., Jiang, L., Wang, X., and Zhao, D. (2017). Combustion Characteristics of Non-premixed Methane Micro-jet Flame in Coflow Air and thermal Interaction between Flame and Micro Tube. *Appl. Therm. Eng.* 112, 296–303. doi:10.1016/j.applthermaleng.2016.10.082

Liu, D., Wall, T., and Stanger, R. (2016). CO_2 Quality Control in Oxy-Fuel Technology for CCS: SO_2 Removal by the Caustic Scrubber in Callide Oxy-Fuel Project. *Int. J. Greenhouse Gas Control.* 51, 207–217. doi:10.1016/j.ijggc.2016.05.026

Liu, F., Guo, H., and Smallwood, G. J. (2003). The Chemical Effect of CO_2 Replacement of N_2 in Air on the Burning Velocity of CH_4 and H_2 Premixed Flames. *Combust. Flame* 133, 495–497. doi:10.1016/s0010-2180(03)00019-1

Luo, W., Wang, Q., Huang, X., Liu, Z., and Zheng, C. (2015). Dynamic Simulation and Transient Analysis of a 3MWth Oxy-Fuel Combustion System. *Int. J. Greenhouse Gas Control.* 35, 138–149. doi:10.1016/j.ijggc.2015.02.003

Mao, Z., Zhang, L., Zhu, X., and Zheng, C. (2017). Experiment Investigation of Coal MILD-Oxy Combustion Integrated with Flue Gas Recirculation at a 0.3MWth Furnace. *Fuel Process. Technol.* 162, 126–134. doi:10.1016/j.fuproc.2017.04.002

Mardani, A., and Fazlollahi Ghomshi, A. (2016). Numerical Study of Oxy-Fuel MILD (Moderate or Intense Low-Oxygen Dilution Combustion) Combustion for CH_4–H_2 Fuel. *Energy* 99, 136–151. doi:10.1016/j.energy.2016.01.016

Maruta, K., Abe, K., Hasegawa, S., Maruyama, S., and Sato, J. (2007). Extinction Characteristics of CH_4/CO_2 versus O_2/CO_2 Counterflow Non-premixed Flames at Elevated Pressures up to 0.7MPa. *Proc. Combust. Inst.* 31, 1223–1230. doi:10.1016/j.proci.2006.08.013

Menage, D., Lemaire, R., and Seers, P. (2018). Experimental Study and Chemical Reactor Network Modeling of the High Heating Rate Devolatilization and Oxidation of Pulverized Bituminous Coals under Air, Oxygen-Enriched Combustion (OEC) and Oxy-Fuel Combustion (OFC). *Fuel Process. Technol.* 177, 179–193. doi:10.1016/j.fuproc.2018.04.025

Moroń, W., and Rybak, W. (2015). Ignition Behaviour and Flame Stability of Different Ranks Coals in Oxy Fuel Atmosphere. *Fuel* 161, 174–181. doi:10.1016/j.fuel.2015.08.065

Oh, J., and Hong, S. (2016). Oxygen Temperature Variation of a Non-premixed Oxy-Methane Flame in a Lab-Scale Slot Burner. *Appl. Therm. Eng.* 104, 804–817. doi:10.1016/j.applthermaleng.2016.05.112

Oh, J., and Noh, D. (2015). Flame Characteristics of a Non-premixed Oxy-Fuel Jet in a Lab-Scale Furnace. *Energy* 81, 328–343. doi:10.1016/j.energy.2014.12.046

Oh, J., Noh, D., and Ko, C. (2013). The Effect of Hydrogen Addition on the Flame Behavior of a Non-premixed Oxy-Methane Jet in a Lab-Scale Furnace. *Energy* 62, 362–369. doi:10.1016/j.energy.2013.09.049

Oh, J., Noh, D., and Lee, E. (2013). The Effect of CO Addition on the Flame Behavior of a Non-premixed Oxy-Methane Jet in a Lab-Scale Furnace. *Appl. Energ.* 112, 350–357. doi:10.1016/j.apenergy.2013.06.033

Oh, J., and Noh, D. (2013). Lifted Flame Behavior of a Non-premixed Oxy-Methane Jet in a Lab-Scale Slot Burner. *Fuel* 103, 862–868. doi:10.1016/j.fuel.2012.09.055

Oh, J., and Noh, D. (2014). The Effect of CO_2 Addition on the Flame Behavior of a Non-premixed Oxy-Methane Jet in a Lab-Scale Furnace. *Fuel* 117, 79–86. doi:10.1016/j.fuel.2013.08.065

OpenFOAM The Open Source CFD Toolbox. 2016 Available at: http://www.openfoam.org.

Rathnam, R. K., Elliott, L. K., Wall, T. F., Liu, Y., and Moghtaderi, B. (2009). Differences in Reactivity of Pulverised Coal in Air (O2/N2) and Oxy-Fuel (O2/CO2) Conditions. *Fuel Process. Technol.* 90, 797–802. doi:10.1016/j.fuproc.2009.02.009

Roper, F. G., Smith, C., and Cunningham, A. C. (1977). The Prediction of Laminar Jet Diffusion Flame Sizes: Part II. Experimental Verification. *Combust. Flame* 29, 227–234. doi:10.1016/0010-2180(77)90113-4

Roper, F. G. (1977). The Prediction of Laminar Jet Diffusion Flame Sizes: Part I.Theoretical Model. *Combust. Flame.* 29, 219–226. doi:10.1016/0010-2180(77)90112-2

Scheffknecht, G., Al-Makhadmeh, L., Schnell, U., and Maier, J. (2011). Oxy-fuel Coal Combustion-A Review of the Current State-Of-The-Art. *Int. J. Greenhouse Gas Control.* 5, S16–S35. doi:10.1016/j.ijggc.2011.05.020

Seddighi, S. (2017). Design of Large Scale Oxy-Fuel Fluidized Bed Boilers: Constant thermal Power and Constant Furnace Size Scenarios. *Energy* 118, 1286–1294. doi:10.1016/j.energy.2016.11.004

Seepana, S., and Jayanti, S. (2012). Experimental Studies of Flame Extinction in a Swirl-Stabilized Oxy-Fuel Burner. *Fuel* 93, 75–81. doi:10.1016/j.fuel.2011.10.065

Seepana, S., and Jayanti, S. (2012). Flame Structure Investigations of Oxy-Fuel Combustion. *Fuel* 93, 52–58. doi:10.1016/j.fuel.2011.07.033

Smith, G. P., Golden, D. M., Frenklach, M., Moriarty, N. W., Eiteneer, B., Goldenberg, M., et al. 2020 Berkeley Mechanical Engineering. Available at: http://www.me.berkeley.edu/gri_mech/.

Taniguchi, M., Yamamoto, K., Okazaki, T., Rehfeldt, S., and Kuhr, C. (2011). Application of Lean Flammability Limit Study and Large Eddy Simulation to Burner Development for an Oxy-Fuel Combustion System. *Int. J. Greenhouse Gas Control.* 5, S111–S119. doi:10.1016/j.ijggc.2011.05.008

Tu, Y., Liu, H., Chen, S., Liu, Z., Zhao, H., and Zheng, C. (2015). Numerical Study of Combustion Characteristics for Pulverized Coal under Oxy-MILD Operation. *Fuel Process. Technol.* 135, 80–90. doi:10.1016/j.fuproc.2014.10.025

Tu, Y., Liu, H., and Yang, W. (2017). Flame Characteristics of CH4/H2 on a Jet-In-Hot-Coflow Burner Diluted by N_2, CO_2, and H_2O. *Energy Fuels* 31, 3270–3280. doi:10.1021/acs.energyfuels.6b03246

Tu, Y., Su, K., Liu, H., Chen, S., Liu, Z., and Zheng, C. (2016). Physical and Chemical Effects of CO_2 Addition on CH_4/H_2 Flames on a Jet in Hot Coflow (JHC) Burner. *Energy Fuels* 30, 1390–1399. doi:10.1021/acs.energyfuels.5b02499

Wall, T. F. (2007). Combustion Processes for Carbon Capture. *Proc. Combustion Inst.* 31, 31–47. doi:10.1016/j.proci.2006.08.123

Wang, J., Matsuno, F., Okuyama, M., Ogami, Y., Kobayashi, H., and Huang, Z. (2013). Flame Front Characteristics of Turbulent Premixed Flames Diluted with CO_2 and H_2O at High Pressure and High Temperature. *Proc. Combust. Inst.* 34, 1429–1436. doi:10.1016/j.proci.2012.06.154

Watanabe, H., Shanbhogue, S. J., Taamallah, S., Chakroun, N. W., and Ghoniem, A. F. (2016). The Structure of Swirl-Stabilized Turbulent Premixed CH_4/air and $CH_4/O_2/CO_2$ Flames and Mechanisms of Intense Burning of Oxy-Flames. *Combust. Flame.* 174, 111–119. doi:10.1016/j.combustflame.2016.09.015

Xie, Y., Wang, J., Zhang, M., Gong, J., Jin, W., and Huang, Z. (2013). Experimental and Numerical Study on Laminar Flame Characteristics of Methane Oxy-Fuel Mixtures Highly Diluted with CO_2. *Energy Fuels* 27, 6231–6237. doi:10.1021/ef401220h

Xu, H., Liu, F., Sun, S., Zhao, Y., Meng, S., and Tang, W. (2017). Effects of H_2O and CO_2 Diluted Oxidizer on the Structure and Shape of Laminar Coflow Syngas Diffusion Flames. *Combust. Flame* 177, 67–78. doi:10.1016/j.combustflame.2016.12.001

Yamamoto, K., Ozeki, M., Hayashi, N., and Yamashita, H. (2009). Burning Velocity and OH Concentration in Premixed Combustion. *Proc. Combust. Inst.* 32, 1227–1235. doi:10.1016/j.proci.2008.06.077

Yin, C., Rosendahl, L. A., and Kær, S. K. (2011). Chemistry and Radiation in Oxy-Fuel Combustion: A Computational Fluid Dynamics Modeling Study. *Fuel* 90, 2519–2529. doi:10.1016/j.fuel.2011.03.023

Zhang, Z., Li, X., Luo, C., Zhang, L., Xu, Y., Wu, Y., et al. (2018). Investigation on the Thermodynamic Calculation of a 35 MWth Oxy-Fuel Combustion Coal-Fired Boiler. *Int. J. Green. Gas Control.* 71, 36–45. doi:10.1016/j.ijggc.2018.02.004

Conflict of Interest: The authors declare that the research was conducted in the absence of any commercial or financial relationships that could be construed as a potential conflict of interest.

Publisher's Note: All claims expressed in this article are solely those of the authors and do not necessarily represent those of their affiliated organizations, or those of the publisher, the editors, and the reviewers. Any product that may be evaluated in this article, or claim that may be made by its manufacturer, is not guaranteed or endorsed by the publisher.